Electronics Letters

LETTER OPEN ACCESS

Linear-Complexity Subcarrier Selection Strategy for Fast Preprocessing of CSI in Passive Wi-Fi Sensing Classification Tasks

Henrique Pires Corrêa[1,2] | Paulo Francisco da Conceição[1,3] | Wilson Conegundes de Freitas Filho[1] | Flávio Rocha[1,2] | Rodrigo Pinto Lemos[1,2]

[1]Excellence Center in Intelligent Wireless Networks and Advanced Services, Federal University of Goiás (CERISE-UFG), Goiânia, Brazil | [2]Federal University of Goiás (UFG), Goiânia, Brazil | [3]Federal Institute of Goiás (IFG), Inhumas, Brazil

Correspondence: Henrique Pires Corrêa (pires_correa@ufg.br)

Received: 21 November 2024 | **Revised:** 30 January 2025 | **Accepted:** 19 March 2025

Funding: The authors received no specific funding for this work.

ABSTRACT

Deployment of low-cost Wi-Fi sensing applications may impose strict constraints on available computational power, thereby making the reduction of time required to process channel state information (CSI) measurements a matter of interest. Most works on passive sensing for classification tasks achieve this via dimensionality reduction of CSI data prior to the training of machine learning models, which in itself still imposes some computational burden. Subcarrier selection, which is a faster approach and is widely used in another application domain (i.e., vital signal monitoring), is seldom considered; in the few works where it is used, only a variance-based unsupervised strategy is applied. In this letter, a supervised linear-complexity subcarrier selection strategy is proposed for enhanced sensing classification accuracy. The approach is validated through practical experiments whose results show that the classification performance can approach or even surpass that obtained via dimensionality reduction, with substantial time savings.

1 | Introduction

The usage of Wi-Fi signals for passive sensing purposes, which is achieved by leveraging channel state information (CSI) that is estimated by receivers as per the IEEE 802.11 standard [1], has been firmly established as a viable procedure in the technical literature. Some noteworthy examples of this approach is its recent applications to: activity recognition [2]; position estimation [3]; fall [4] and intrusion detection [5]; heartbeat [6] and respiration monitoring [7]; and materials identification [8]. Such a wide range of useful applications, coupled with the development and imminent release of a sensing-oriented amendment to the Wi-Fi standard (i.e., the 802.11bf protocol) [9], indicates a near future with widespread commercial sensing implementations.

In general, Wi-Fi sensing methods use machine learning (ML) to make inferences from CSI data. Since most implementations are expected to be carried out with low-cost hardware (i.e., Internet of Things devices or user-grade computers with off-the-shelf network cards) [10], it is critical to ensure that training the ML models does not demand excessive computational resources. Two preprocessing approaches commonly used in sensing for reducing the computational burden are dimensionality reduction and subcarrier selection [11]. The former consists of applying a linear projection technique (in most cases, principal component analysis - PCA; see [12]), whereas the latter employs a given heuristic to select a subset of subcarriers whose CSI values will feed the ML model (e.g., as in [13, 14]). Dimensionality reduction entails relatively costly matrix computations, and thus

using subcarrier selection is of interest if processing time is deemed critical.

Subcarrier selection is mostly employed for vital signal monitoring applications, in which the basic principle is using the training data to compute CSI variance for each subcarrier and, subsequently, selecting a given number of subcarriers with the *largest* variances (which indicate greater sensitivity to the vital signal) for further processing. Existing strategies mostly differ with respect to complementary criteria (i.e., other than variance) used during selection; for instance, spectral stability [15], periodicity [16] and vital signal energy ratio [17] may be assessed.

Contrastingly, very few classification-oriented applications (such as activity recognition) use subcarrier selection and those which do are based on the simplistic unsupervised strategy of selecting a number of subcarriers with the smallest CSI variances (e.g., [18, 19]) for improving classification accuracy. Despite its proven effectiveness, this approach does not consider two important aspects during the selection process, namely: (i) the available class labels, which can be leveraged to evaluate inter-class variance and (ii) the correlation between adjacent-frequency subcarriers, which reduces mutual information. Taking this into account, this letter proposes a linear-complexity supervised strategy considering such factors in order to improve sensing accuracy when the subcarrier selection approach is used for classification tasks.

2 | Preliminaries

The 802.11 receiver computes CSI for each incoming packet (physical protocol data unit - PPDU), which is an estimate of the frequency response (amplitude and phase) of the wireless channel at given frequencies, namely those of the orthogonal frequency division multiplexing (OFDM) subcarriers. For subcarrier i with frequency f_i in the multiple input multiple output (MIMO) stream j, we have [20]:

$$R_j(f_i) = H_{ij} \cdot S(f_i) + N_j(f_i) \Rightarrow H_{ij} \approx \frac{R_j(f_i)}{S(f_i)} \tag{1}$$

where $S(f_i)$ is the transmitted OFDM symbol at f_i of a training sequence, $R_j(f_i)$ is the corresponding received symbol, $N_j(f_i)$ denotes noise and $H_{ij} \in \mathbb{C}$ is the estimated CSI of subcarrier i in the j-th MIMO stream. If there are M_1 subcarriers and M_2 streams, then a CSI vector $\boldsymbol{x} = [x_i]_{1\times M} = [H_{11}\ H_{12} \cdots H_{1M_1}\ H_{21}\ H_{22} \cdots H_{2M_1} \cdots H_{M_2M_1}]$ of dimension $M = M_2M_1$ is computed for every PPDU. Now, if N PPDUs are received, $\boldsymbol{X} = [X_{ij}]_{N\times M} = [\boldsymbol{x}_1^\top\ \boldsymbol{x}_2^\top \cdots \boldsymbol{x}_N^\top]^\top$ is the CSI data matrix that must be preprocessed and used to train the ML model; at last, for classification tasks, a label vector $\boldsymbol{y} = [y_i]_{N\times 1}$ accompanies matrix $\boldsymbol{X}$ and indicates to which class each of the PPDUs belongs [21].

It has been shown that adequate accuracy can be obtained in static scenarios (i.e., no class y_i refers to a time-varying event) by carrying out classification on a packet-by-packet basis [22]. On the other hand, proper classification of dynamic events requires additional processing prior to the ML input. In this case, the full CSI data are naturally segmented as $\boldsymbol{X} = [\boldsymbol{X}_1^\top\ \boldsymbol{X}_2^\top \cdots \boldsymbol{X}_P^\top]^\top$, with $\boldsymbol{X}_i = [X_{ij}]_{Q\times M}$ and $N = PQ$; each matrix $\boldsymbol{X}_i$ corresponds to some fixed

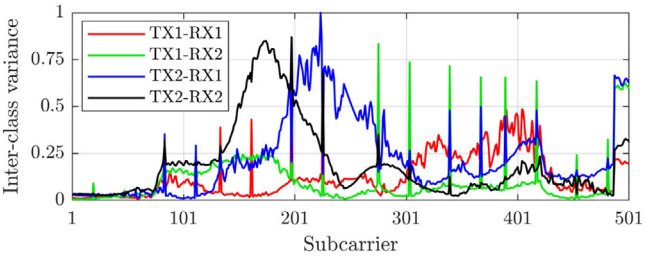

(a) Inter-class amplitude variance for different MIMO streams.

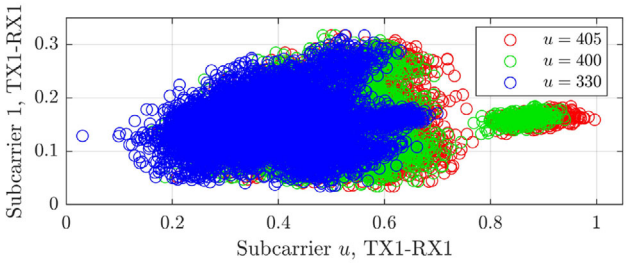

(b) Amplitude scatter plots with subcarrier 1 as reference.

FIGURE 1 | Inter-class variance and scatter plots of CSI amplitude data.

y_i and Q is the event window. A feature extractor $h : \mathbb{C}^{Q\times M} \to \mathbb{C}^{1\times H}$ is applied to each $\boldsymbol{X}_i$ to generate H-dimensional feature vectors $\boldsymbol{x}'_i = h(\boldsymbol{X}_i)$, which compose a matrix $\boldsymbol{X}' = [X'_{ij}]_{P\times H} = [\boldsymbol{x}_1'^\top\ \boldsymbol{x}_2'^\top \cdots \boldsymbol{x}_P'^\top]^\top$ that feeds the ML algorithm [3].

Note that, since CSI phase (recall that $H_{ij} \in \mathbb{C}$) is inherently noisy and requires more elaborate preprocessing techniques to be usable, many methods simply opt to only use the amplitude [23]. Since we aim at a low-complexity method, such approach is henceforth adopted. However, all theoretical considerations that follow are applicable to CSI phase.

3 | Motivation

To expose the intuition that motivates this work, we present in Figure 1a,b, respectively, the inter-class amplitude variance for each 2×2 MIMO stream of a 160 MHz system ($M_1 = 501$ subcarriers) and a corresponding scatter plot of the subcarrier 1 amplitude against that of different subcarriers (denoted as u). These plots are normalized and pertain to the data collected in an experiment to be described further in this letter, and comprise a total of 9300 PPDUs and seven classes.

Let Σ_u^2 be the variance of subcarrier u, which is decomposed into intra-class (Σ_{u0}^2) and inter-class (σ_u^2) variances as $\Sigma_u^2 = \Sigma_{u0}^2 + \sigma_u^2$. At first, it is clear that the usual preprocessing approach of selecting u such that Σ_u^2 is minimized does not ensure optimality for classification, since class separability is associated with maximizing σ_u^2. An optimal selection will only be made if $\Sigma_{u0}^2 \gg \sigma_u^2$, which cannot be ascertained a priori.

Aside from the above consideration, we now consider the problem of subcarrier correlation. Referring to Figure 1a,b and focusing on stream TX1-RX1 and subcarriers $u = 330, 400, 405$ (all of which are local maxima in the inter-class variance plot), it is

seen that $\sigma^2_{330} < \sigma^2_{400}$ and $\sigma^2_{330} < \sigma^2_{405}$. Despite this fact, it is clear from the scatter plot that subcarriers 400 and 405 are strongly correlated and therefore redundant; subcarrier pairs $\{330, 400\}$ and $\{330, 405\}$ both explain the CSI data better than the pair $\{400, 405\}$. It is thus clear that, aside from interclass variance, correlation between the CSI of different subcarriers is relevant and should be considered in the subcarrier selection process.

The subcarrier selection strategy proposed in what follows aims at tackling the above problems to improve classification performance while maintaining a relatively small computational complexity.

4 | Proposed Strategy

It is proposed that supervised subcarrier selection be carried out as follows. Two integer parameters are first chosen: the number of subcarriers to be selected per stream (K) and the minimum subcarrier spacing (Δ). Now, each σ_i^2, $i = 1, 2, \ldots, M$ is computed for the training set $\boldsymbol{X}_{\text{tr}}$, with aid of the label vector $\boldsymbol{y}_{\text{tr}}$. In particular, we note that if feature extraction is used, σ_i^2 is computed over the space of extracted features for subcarrier i in $\boldsymbol{X}'_{\text{tr}}$. Then, ordered sets $\mathcal{I}_j$ of subcarrier indices, $j = 1, 2, \ldots, M_2$ (one per MIMO stream), are formed, with an order relation of decreasing σ_i^2. At last, for each $\mathcal{I}_j$, the following algorithm is used to populate a selection set $\mathcal{S}_j$:

1. Set $k = 1$ and $\mathcal{S}_j = \emptyset$;
2. $\mathcal{S}_j \leftarrow \mathcal{S}_j \cup \mathcal{I}_j(k)$;
3. $k \leftarrow k + 1$;
4. If $k > M_1$ or $\#\mathcal{S}_j = K$, go to Step 6;
5. If $\min_u |k - \mathcal{I}_j(u)| \geq \Delta$ and $\#\mathcal{S}_j < K$, then go to Step 2. In other case, go to Step 3;
6. Return $\mathcal{S}_j$.

In the above algorithm, $\mathcal{I}_j(k)$ is the k-th element of ordered set $\mathcal{I}_j$ and $\#\mathcal{S}_j$ is the number of elements in $\mathcal{S}_j$. As a last step, the final set of selected subcarriers is obtained as $\mathcal{S} = \bigcup_{j=1}^{M_2} \mathcal{S}_j$. Put simply: for each stream, the subcarriers with greatest inter-class variance are selected, except when a candidate subcarrier violates a minimum spacing criterion and is thus excluded. An equal number K of subcarriers is selected from each stream, which is done to leverage space diversity in a simple manner [24]; the total number of selected subcarriers is thus KM_2.

To explain why the spacing mechanism implemented via Δ is expected to improve sensing accuracy, recall that wireless channels are subject to multipath propagation and can thus be modelled by a frequency response with some coherence bandwidth B_c [25]. A pair of subcarriers i and j such that $|i - j| \cdot \delta f < B_c$, where δf is the OFDM subcarrier spacing, is expected to present high coherence and, as a consequence, redundancy. Hence, Δ prevents neighbouring subcarriers to be selected based solely on inter-class variance, which would otherwise very likely happen precisely due to their coherence (and thus similar variances).

In principle, we could compute the Pearson correlation coefficients between each pair of subcarriers in each stream and use them to obtain $\mathcal{S}$. However, this approach entails a quadratic computational complexity of $O(NM_1^2M_2)$, corresponding to the computation of M_2 covariance matrices, each with N data points of dimension M_1. On the other hand, the proposed method has a linear complexity of $O(NM_1M_2)$, since it only requires computing inter-class variance of M_1M_2 subcarriers. As we aim at low complexity, the Δ-based approach is more expedient.

For further comparison, dimensionality reduction with either PCA or linear discriminant analysis (LDA, which is a supervised method) would imply a complexity $O(NM^2 + M^3) = O(NM_1^2M_2^2 + M_1^3M_2^3)$ [26]. In a further section, the relative preprocessing time benefit yielded by the linear complexity of the proposed method will become clear.

We note that, for simplicity, K and Δ have been assumed as given thus far. In the subsequent section, we suggest straightforward strategies for selecting such parameters in case trial-and-error is deemed undesirable.

5 | Parameter Selection

The value of K determines the amount of features that are used for training the ML algorithm, which entails a trade-off between computational burden and classification accuracy. Hence, if an automated selection of K is desired, we propose that it be carried out by assessing the fraction α of explained CSI inter-class variance as a function of K. In other words, let σ^2_{total} and α_{th} be the total inter-class variance (i.e., for $K = M_2$) and a desired threshold, respectively. Then, K is selected as the smallest value that satisfies $\alpha(K, \sigma^2_{\text{total}}) \geq \alpha_{\text{th}}$.

A data-driven selection of Δ would not be as straightforward since, as mentioned in the previous section, CSI correlation between adjacent subcarriers is mainly a function of environment multi-path propagation properties [25]. Hence, to leverage this important physical significance, it is proposed that the heuristic $\Delta > B_c/\delta f$ be used for selecting Δ by employing typical tabulated values of coherence bandwidth B_c.

At last, we note that, to ensure that K subcarriers with a minimum spacing of Δ can always be selected, $K\Delta < M_1$ must be satisfied.

6 | Validation

To evaluate the proposed method, indoor experiments involving the task of jointly classifying human position and activity are considered. Both static and dynamic scenarios are taken into account, with packet-wise classification being carried out in the former case and feature extraction in the latter (as discussed in a previous section). We now describe the general setup common to both considered scenarios.

The designed indoor sensing problem, which is illustrated in Figure 2, consists in discriminating between different classes which correspond to possible combinations of human positions and activities; an additional class associated to no human pres-

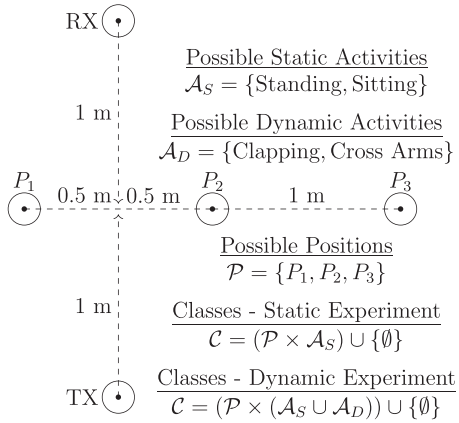

FIGURE 2 | Illustration of the sensing scenario.

ence is also included. In the static case, three positions and two activities (standing and sitting) are considered, whereas the dynamic scenario includes two additional activities which are, of course, time-varying (clapping hands and crossing arms).

A 2×2 MIMO link is considered that consists of two AX-210 network cards operating at a carrier frequency of 6.0125 GHz, with 160 MHz and 312.5 kHz channel and subcarrier bandwidths, respectively ($M_1 = 501$, $M_2 = 4$). For each of the sensing classes, PPDUs are transmitted over the link at a rate R (specified later) over a 30 s time period; this process is repeated for five volunteers (except for the no-presence class). The PicoScenes tool [27] was used to set up the link and extract CSI values.

The proposed approach is used to preprocess the collected CSI data prior to a support vector machine (SVM) classifier with regularization parameter $C = 1$ and radial basis function kernel. Its performance is compared, in terms of run time and classification accuracy (evaluated via tenfold cross-validation), against that obtained with PCA, LDA and the ordinary unsupervised subcarrier selection approach.

7 | Static Experiment - First Part

For the static scenario, the selected PPDU rate is $R = 10$ Hz; a total of $N = 9300$ PPDUs were collected. In this first part of the experiment, we select $\Delta = 8$ based on the previously proposed heuristic (which yields $\Delta > 7$ for the typical indoor coherence bandwidth $B_c \approx 2.3$ MHz [28]) and performances are evaluated for $K = 1, 3, 6, \ldots, 45$. Note that, for PCA and LDA, K stands for the number of features in the transformed domain per MIMO stream (whereas, in subcarrier selection, it is simply the number of selected subcarriers). The effect on accuracy due to varying Δ and selecting K based on explained variance will be examined in the second part of this experiment.

Obtained results are depicted in Figure 3, where t_{method} and a_{method} denote the run time and accuracy of a given preprocessing method; the unsupervised subcarrier selection approach and the proposed method are denoted by SCS and SCS_p, respectively. For further comparison, we also present the values of T_{SVM}, which is the average, taken over all of the preprocessing methods, of measured SVM training time.

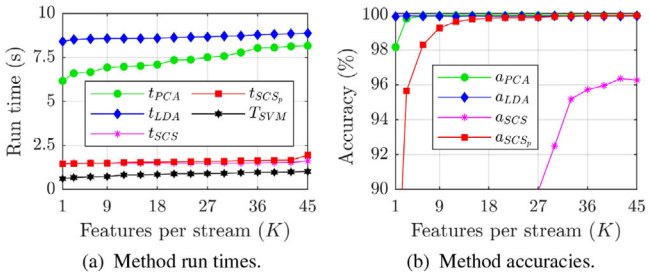

FIGURE 3 | Comparison of run time and accuracy for different methods.

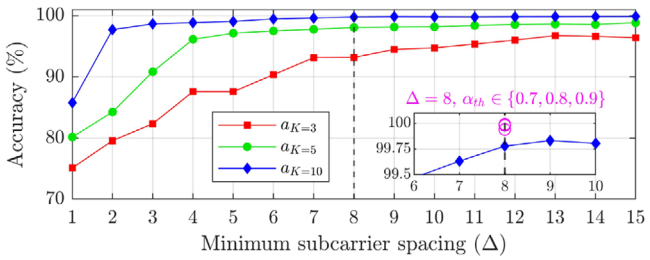

FIGURE 4 | Accuracy of the proposed method in terms of subcarrier spacing.

The results make it clear that the proposed method successfully reduces overall run time compared to PCA and LDA. On average, these latter methods yielded $(T_{\text{SVM}} + t_{\text{PCA,LDA}})/T_{\text{SVM}} > 10$, which shows an order of magnitude increase due to preprocessing. This is not the case for the proposed approach, for which $(T_{\text{SVM}} + t_{\text{SCS}_p})/T_{\text{SVM}} < 3$ on average. It is relevant to note that such results are in agreement with the computational complexity analysis carried out in a previous section.

With regard to accuracy, it is seen that, for sufficiently large K, the proposed method converges to the performance of PCA and LDA. This is a theoretically sound result: since PCA and LDA compress most of the CSI variance into the dominant components of the transformed domain, their accuracies are indeed expected to converge faster in K. In any case, a satisfactory convergence is achieved by the proposed method due to its usage of weakly correlated subcarriers. This point becomes clear via comparison to standard subcarrier selection: since it does not mitigate subcarrier correlation, its accuracy convergence is poor.

8 | Static Experiment - Second Part

For a more comprehensive analysis, the same data of the previous section is used for assessing the accuracy yielded by the proposed approach for different values of the minimum subcarrier spacing, namely $\Delta = 1, 2, \ldots, 15$. Such evaluation is carried out with $K = 2, 5, 10$; these values of K are considered since Figure 3 shows that accuracy is already close to convergence at $K = 9$. Finally, we also evaluate the accuracy obtained by using $\Delta = 8$ with the proposed data-driven selection of K for thresholds $\alpha_{\text{th}} = 0.7, 0.8, 0.9$.

The results are given in Figure 4, where $a_{K=\omega}$ denotes the accuracy for $K = \omega$. As already expected from previous analysis, it is seen that larger K yields better performance for a given Δ. More

importantly, it is clear that larger Δ values enable the achievement of greater accuracy for a fixed number of subcarriers K. This fact highlights an interesting advantage of the proposed method: by increasing Δ, accuracy can be maintained with smaller K and thus with less computational burden. On the other hand, Δ may not be increased arbitrarily: by recalling that $K\Delta < M_1$, we see that an exceedingly large Δ will greatly reduce the maximum allowable value of K, which leads to decreased accuracy.

It is seen that convergence of accuracy in Δ is faster for larger K, which can be explained by the fact that more subcarriers yield better frequency diversity (and thus improved decorrelation) even when Δ is small. Note that convergence for $K = 2$ begins at $\Delta \approx 8$. This fully agrees with the proposed heuristic for selecting Δ (recall that it resulted in $\Delta = 8$ in the previous section), that is, two subcarriers ($K = 2$) with indices i and j become approximately decorrelated for $|i - j| > 7$.

At last, consider the accuracies obtained by means of data-driven selection of parameter K. Comparison of such results with the $a_{K=10}$ curve make it particularly clear that the proposed approach managed to compute K values for which accuracy convergence is ensured. It must be noted, however, that adequate performance can be obtained with smaller values of K than those computed via data-driven selection. In fact, the selected parameter values (for increasing α_{th}) were $K = 26, 32, 40$.

9 | Dynamic Experiment

For the dynamic scenario, we select $R = 100$ Hz and an event window of $Q = 300$, which corresponds to 3 s events; a total of $N = 183,000$ PPDUs were captured in this experiment. The feature extractor h computes the mean, standard deviation, and skewness for each subcarrier amplitude. Hence, it is a map $h : \mathbb{R}^{300\times2004} \to \mathbb{R}^{1\times6012}$ and the feature matrix $\boldsymbol{X}'$ dimensions are thus $P = 610$ and $H = 6012$.

Aside from enabling the evaluation of time-varying activities, this experiment is also relevant due to it being representative of the small sample size problem ($H > P$) introduced by feature extraction over the event window. In such circumstances, PCA is known to have worsened performance due to the effective dimensionality of its transformed domain being limited to P [29], whereas LDA is prone to divergence due to severe ill-conditioning of its within-class scatter matrix [30].

We proceed as in the first part of the static experiment and evaluate the performances of each method for $K = 1, 3, 6, \ldots, 45$ and $\Delta = 8$; additionally, we evaluate the proposed data-driven selection of K for $\alpha_{\text{th}} = 0.7, 0.8, 0.9$. Obtained results are given in Figure 5, where we only display accuracy data since run time results were very similar to those already analysed for the static experiment. The LDA approach is not shown because, in agreement with the above discussion, it diverged for all K. At last, the confusion matrix for proposed method with $K = 45$ is given in Figure 6, where the following acronyms are used for the activities: St (standing), Si (sitting), Cl (clapping hands), Cr (crossing arms).

It is remarkable that the proposed approach consistently surpassed the accuracy of PCA, with a single exception at $K = 9$.

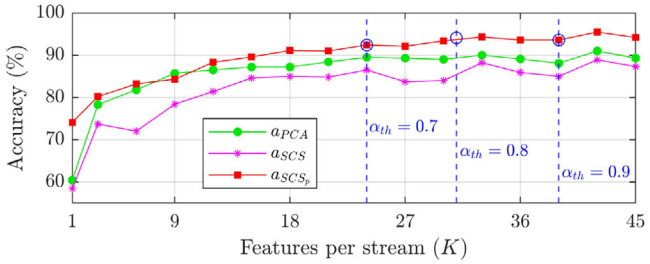

FIGURE 5 | Comparison of accuracy for different methods in dynamic scenario.

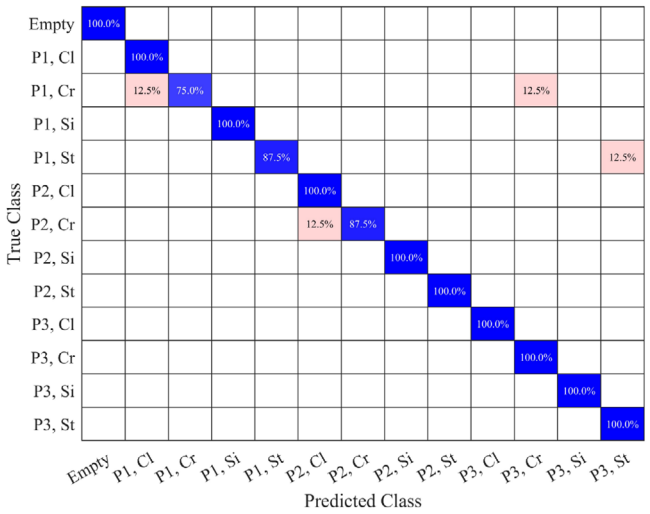

FIGURE 6 | Confusion matrix for the proposed method ($K = 45$).

This result can be considered consistent with the above discussion on small sample size: Since PCA is forced to compress data variance into a lower-dimensional transformed domain, its larger eigenvalues become less dominant and more information is lost in the discarded principal components. The proposed method has no such limitation, since its computations are subcarrier-wise and not constrained by the number of samples.

We observe that, similarly to previous results, (i) ordinary subcarrier selection consistently remains as the underperforming method and (ii) the proposed data-driven selection of K successfully obtained parameter values ($K = 24, 31, 39$) which yield satisfactory convergence. At last, it is of interest to notice, in Figure 6, that all classification errors pertain either to a common activity or position. This is an intuitively satisfactory result, as CSI patterns associated to a change only in location or activity must have greater similarity than when both factors are altered.

10 | Conclusion

A novel subcarrier selection method applicable to classification-oriented tasks in Wi-Fi sensing was proposed. Differently from an often-used unsupervised approach, it leverages class labels to achieve a supervised selection based on inter-class variance and employs a minimum subcarrier spacing scheme to prevent redundancy of CSI data. Compared to dimensionality reduction-based approaches, it has an advantageous linear computational com-

plexity. Validation was carried out by experiment, whose results show that the proposed method yields significant preprocessing time savings and converges to accuracies either comparable or better than those obtained with dimensionality reduction.

Author Contributions

Henrique Pires Corrêa: conceptualization, supervision, writing – original draft. **Paulo Francisco da Conceição**: investigation, methodology, software. **Wilson Conegundes de Freitas Filho**: investigation, methodology, software. **Flávio Rocha**: investigation, writing – review and editing. **Rodrigo Pinto Lemos**: investigation, writing – review and editing.

Acknowledgements

This work has been supported by the Excellence Center in Intelligent Wireless Networks and Advanced Services (CERISE- UFG). The authors would like to thank the volunteers for dispensing their time towards participation in the data collection process.

Conflicts of Interest

The authors declare no conflicts of interest.

Data Availability Statement

The data supporting this study are available from the corresponding author upon reasonable request.

References

1. "IEEE Standard for Information Technology - Telecommunications and Information Exchange between Systems - Local and Metropolitan Area Networks - Specific Requirements - Part 11: Wireless LAN Medium Access Control (MAC) and Physical Layer (PHY) Specifications," in *IEEE Std 802.11-2020, Revision of IEEE Std 802.11-2012* (IEEE, 2021), 1–76.

2. X. Lu, Y. Li, W. Cui, et al., "CeHAR: CSI-Based Channel-Exchanging Human Activity Recognition," *IEEE Internet of Things Journal* 10, no. 7 (2023): 5953–5961.

3. Y. Zhang, D. Li, and Y. Wang, "An Indoor Passive Positioning Method Using CSI Fingerprint Based on Adaboost," *IEEE Sensors Journal* 19, no. 14 (2019): 5792–5800.

4. Z. Xia and S. Chong, "WiFi-Based Indoor Passive Fall Detection for Medical Internet of Things," *Computers and Electrical Engineering* 109, no. B (2023): 108763.

5. T. Wang, D. Yang, S. Zhang, Y. Wu, and S. Xu, "Wi-Alarm: Low-Cost Passive Intrusion Detection Using WiFi," *Sensors* 19, no. 10 (2019).

6. J. Sun, X. Bian, and M. Li, "Non-Contact Heart Rate Monitoring Method Based on Wi-Fi CSI Signal," *Sensors* 24, no. 7 (2024).

7. W. Xie, L. Gan, L. Huang, et al., "A Real-Time Respiration Monitoring System Using WiFi Sensing Based on the Concentric Circle Model," *IEEE Transactions on Biomedical Circuits and Systems* 17, no. 2 (2023): 157–168.

8. D. Zhang, J. Wang, J. Jang, et al., "On the Feasibility of Wi-Fi Based Material Sensing," in *The 25th Annual International Conference on Mobile Computing and Networking* MobiCom '19, (Association for Computing Machinery, 2019), 1–16.

9. R. Du, H. Hua, H. Xie, et al., "An Overview on IEEE 802.11bf: WLAN Sensing," *IEEE Communications Surveys and Tutorials* 27, no. 1 (2024): 184–217.

10. S. M. Hernandez and E. Bulut, "Wi-Fi Sensing on the Edge: Signal Processing Techniques and Challenges for Real-World Systems," *IEEE Communications Surveys and Tutorials* 25, no. 1 (2023): 46–76.

11. J. A. Armenta-Garcia, F. F. Gonzalez-Navarro, and J. Caro-Gutierrez, "Wireless Sensing Applications With Wi-Fi Channel State Information, Preprocessing Techniques, and Detection Algorithms: A Survey," *Computer Communications* 224 (2024): 254–274.

12. Y. Tian, C. Chen, Q. Zhang, et al., "Multidimensional Information Recognition Algorithm Based on CSI Decomposition," *IEEE Internet of Things Journal* 10, no. 10 (2023): 9234–9248.

13. T. Deng, B. Zheng, R. Du, F. Liu, and T. X. Han, "A Statistical Sensing Method by Utilizing Wi-Fi CSI Subcarriers: Empirical Study and Performance Enhancement," *Journal of Information and Intelligence* 2, no. 4 (2024): 365–374.

14. R. Zhang, Z. Wang, G. Li, et al., "Hybrid Subcarrier Selection Method for Vital Sign Monitoring With Long-Term and Short-Term Data Considerations," *IEEE Sensors Journal* 22, no. 23 (2022): 23209–23220.

15. A. Khamis, C. T. Chou, B. Kusy, and W. Hu, "Cardiofi: Enabling Heart Rate Monitoring on Unmodified Cots WiFi Devices," in *Proceedings of the 15th EAI International Conference on Mobile and Ubiquitous Systems: Computing, Networking and Services MobiQuitous '18* (Association for Computing Machinery, 2018), 97–106.

16. X. Liu, J. Cao, S. Tang, and J. Wen, "Wi-Sleep: Contactless Sleep Monitoring via WiFi Signals," in *Proceedings of the 2014 IEEE Real-Time Systems Symposium* (IEEE, 2014), 346–355.

17. Z. Guo, W. Yuan, L. Gui, B. Sheng, and F. Xiao, "Breatheband: A Fine-Grained and Robust Respiration Monitor System Using WiFi Signals," *ACM Transactions on Sensor Networks* 19, no. 4 (2023): 1–18, https://doi.org/10.1145/3582079.

18. M. Peng, B. Ge, X. Fu, and C. Kai, "Wi-Tar: Object Detection System Based on CSI Ratio," *IEEE Sensors Journal* 24, no. 10 (2024): 16540–16550.

19. W. Taylor, M. Z. Khan, A. Tahir, et al., "An Implementation of Real-Time Activity Sensing Using Wi-Fi: Identifying Optimal Machine-Learning Techniques For Performance Evaluation," *IEEE Sensors Journal* 22, no. 21 (2022): 21127–21134.

20. W. Li, M. J. Bocus, C. Tang, et al., "A Taxonomy Of Wifi Sensing: Csi Vs Passive Wifi Radar," in *Proceedings of the 2020 IEEE Globecom Workshops* (IEEE, 2020), 1–6.

21. Y. Ma, G. Zhou, and S. Wang, "WiFi Sensing With Channel State Information: A Survey," *ACM Computing Surveys* 52, no. 3 (2019): 1–36.

22. D. Mendez, M. Zennaro, M. Altayeb, and P. Manzoni, "On TinyML WiFi Fingerprinting-Based Indoor Localization: Comparing RSSI vs. CSI Utilization," in *2024 IEEE 21st Consumer Communications and Networking Conference (CCNC)* (2024), 1–6.

23. V. V. Ratnam, H. Chen, H.-H. Chang, A. Sehgal, and J. Zhang, "Optimal Preprocessing of WiFi CSI for Sensing Applications," *IEEE Transactions on Wireless Communications* 23, no. 9 (2024): 10820–10833.

24. K. Qian, C. Wu, Z. Yang, Y. Liu, F. He, and T. Xing, "Enabling Contactless Detection of Moving Humans With Dynamic Speeds Using CSI," *ACM Transactions on Embedded Computing Systems* 17, no. 2 (2018): 52.

25. T. S. Rappaport, *Wireless Communications: Principles and Practice*, Prentice Hall Communications Engineering and Emerging Technologies Series (Prentice Hall PTR, 2002).

26. A. Tharwat, T. Gaber, A. Ibrahim, and A. E. Hassanien, "Linear Discriminant Analysis: A Detailed Tutorial," *AI Communications* 30 (2017): 169–190.

27. R. Li, Y. Duan, R. Du, et al., "Reshaping WiFi ISAC With High-Coherence Hardware Capabilities," *IEEE Communications Magazine* 62, no. 9 (2024): 114–120.

28. S. Farahani, "RF Propagation, Antennas, and Regulatory Requirements," in *ZigBee Wireless Networks and Transceivers*, ed. S. Farahani, (Springer, 2008), 171–206.

29. M. Pechenizkiy, S. Puuronen, and A. Tsymbal, "The Impact of Sample Reduction on PCA-Based Feature Extraction for Supervised Learning," in

Proceedings of the 2006 ACM Symposium on Applied Computing SAC '06, (Association for Computing Machinery, 2006), 553–558.

30. L. Qu and Y. Pei, "A Comprehensive Review on Discriminant Analysis for Addressing Challenges of Class-Level Limitations, Small Sample Size, and Robustness," *Processes* 12, no. 7 (2024): 1382, https://doi.org/10.3390/pr12071382.